www.MaterialsViews.com

ADVANCED
FUNCTIONAL
MATERIALS
www.afm-journal.de

FULL PAPER

Membrane-Based Self-Powered Triboelectric Sensors for Pressure Change Detection and Its Uses in Security Surveillance and Healthcare Monitoring

Peng Bai, Guang Zhu, Qingshen Jing, Jin Yang, Jun Chen, Yuanjie Su, Jusheng Ma, Gong Zhang, and Zhong Lin Wang*

A new membrane-based triboelectric sensor (M-TES) is presented as a self-powered pressure change sensor. It generates a voltage induced by surface triboelectric charges in response to an air pressure change. Extremely high detection resolutions of 0.34 Pa and 0.16 Pa are achieved when the air pressure increases and decreases in a small region away from the ambient standard atmosphere pressure, respectively, indicating an excellent sensitivity. By integrating the M-TES with a signal processing unit, we demonstrate practical applications of the device in sensing footsteps, respirations, and heartbeat, which suggests widespread use of the M-TES in fields of security surveillance, chemical engineering, geography research, environment monitoring, and personal healthcare.

1. Introduction

Air pressure sensors have been widely used in specific applications such as pressure sensing, altitude sensing, flow sensing, depth sensing, and leakage detection.[1–3] Multiple mechanisms, such as piezoelectric,[4] piezoresistive,[5] capacitive,[6] and optical[7] techniques have been used for this purpose. However, most of these techniques require complicated and expensive instrumentation as well as time-consuming processes for device fabrication, and need an external power supply to generate measurable electric signals, which precludes widespread practical applications.[8,9] To overcome these limitations, self-powered sensors that can generate electric signals without relying on external power sources have been reported,[10,11]

such as recently emerged triboelectric sensors.[12–14] Triboelectric sensors take advantage of the triboelectric effect and provides an effective way of converting mechanical energy into electricity.[15–18] Repeated contact and separation between two dissimilar materials that have different triboelectric polarities can create a periodically changing electric potential difference between two electrodes, which can drive electrons to flow through external loads. Modified surface morphologies in micro/nano scale, such as nanowires,[19] nanoparticles,[20] and nanopores[21] have been demonstrated to improve the electric output. Therefore, the triboelectric sensor emerges as a promising approach for active self-powered sensing.

Here in this work, we report a new membrane-based triboelectric sensor (M-TES) as a self-powered approach for air pressure change sensing, surveillance, and health monitoring. Having small dimensions of 3.7 cm by 3.7 cm by 0.2 cm and a light weight of 7 g, the M-TES can be utilized wherever the air pressure changes. High resolutions of 0.34 Pa and 0.16 Pa are achieved when the air pressure increases and decreases respectively. Higher sensitivity can be obtained if the device is further miniaturized. As a result of the robust design, excellent stability is realized. Furthermore, the M-TES can effectively respond the pressure change caused by human footsteps, respirations and even heartbeats without an external power supply. Therefore, this work presents practical applications of the M-TES in fields of security surveillance, chemical engineering, geography research, and environment monitoring.

P. Bai, Prof. J. Ma, Prof. G. Zhang
Department of Mechanical Engineering
Tsinghua University
Beijing 100084, China
P. Bai, Dr. G. Zhu, Q. Jing, J. Yang, J. Chen, Y. Su,
Prof. Z. L. Wang
School of Materials Science and Engineering
Georgia Institute of Technology
Atlanta, Georgia 30332–0245, United States
E-mail: zlwang@gatech.edu
Dr. G. Zhu, Prof. Z. L. Wang
Beijing Institute of Nanoenergy and Nanosystems
Chinese Academy of Sciences
Beijing, China

2. Results and Discussion

The M-TES has a multi-layered structure which is schematically illustrated in **Figure 1**a. A piece of acrylic sheet with a thickness of 1.6 mm was prepared by laser cutting as a substrate. One layer of copper with a thickness of 100 nm was deposited on the substrate as a circular top electrode (a diameter of 2.0 cm) while another layer of copper was deposited on the back of the substrate as a back electrode. Then, a 125-µm-thick fluorinated ethylene propylene (FEP) film was securely attached
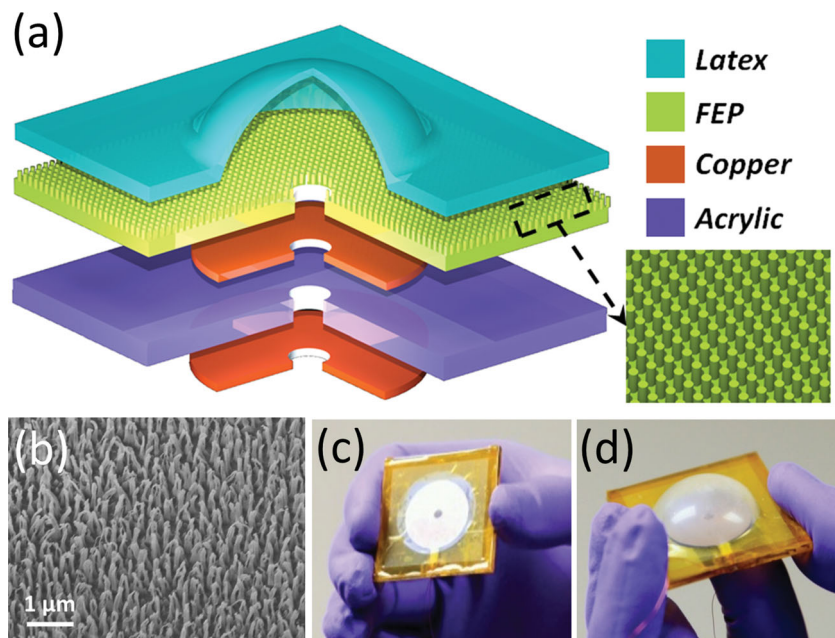
Figure 1. (a) Schematic of the M-TES. (b) SEM image of FEP nanorod arrays. (c) Photograph of an M-TES and (d) an M-TES with the latex membrane swelling.

onto the top electrode. A through air-conducting channel with a diameter of 2.0 mm was created at the center of the device. A latex membrane with a thickness of 50 μm was brought to a plane-plane intimate contact with the FEP film. Epoxy resin was used to seal the edges between the membrane and the FEP surface to prevent any air leakage. To promote the sensitivity of the M-TES, vertically aligned FEP nanorod (NR) arrays were created on the FEP surface by a top-down dry etching technique,[22] as shown in the inset of Figure 1a. As revealed by a scanning electron microscopy (SEM) image in Figure 1b, the FEP NRs are uniformly distributed on the surface of the FEP film after being etched for five minutes. They have an average diameter of 130 nm and a length of 500 nm. Figure 1c exhibits a photograph of the M-TES with a circular apparent contact area of 3.2 cm². In response to a pressure change from the air-conducting channel, the latex membrane will swell, resulting in a separation away from the FEP film (Figure 1d).

The operating principle of an M-TES is schematically illustrated in **Figure 2**. All of the schematics in this figure are plotted in two-dimensional cross-sectional view without showing the NRs. At the initial state, the latex membrane is in contact with the FEP film. Due to the different triboelectric polarities between these two materials,[23] negative charges will be injected from the latex membrane to the FEP film (Figure 2a). Because of the law of charge conservation, the density of positive charges (σ) on the latex is the same as that of negative ones on the FEP. In open-circuit condition, electrons cannot transfer between electrodes; and the triboelectric charges are uniformly distributed on the surfaces at macro scale with negligible decay.[24,25] Once a pressure change occurs from the air-conducting channel, the latex membrane will begin to swell and separate from the FEP due to deformation, forming an arc-shaped air cavity in between. The maximum distance between the membrane and the FEP surface occurs at the center of the

device (Figure 2b). Such a separation results in a potential difference established between the two electrodes (Figure 2e), which is caused by the electric field leakage at the edges of the finite-sized electrodes.[26,27] The potential difference will reach its maximum value when the pressure of the air cavity and the ambient pressure reach an equilibrium (Figure 2c and 2e). If the air pressure drops, the membrane starts to approach the FEP film due to its elasticity. Then, the electric potential difference will decrease from the maximum value back to zero until a fully contact is achieved again (Figure 2d and 2e). Therefore, the M-TES is capable of dynamic air pressure change sensing. If we assume that the air is an ideal gas and the change of air pressure is isothermal, the air pressure change (ΔP) can be calculated as below:

$$\Delta P = P - P_0 = P_0(W_0 - W)/W \tag{1}$$

where P is the air pressure after changing, P_0 is the original air pressure that is approximated by the standard atmospheric pressure (101.3 KPa), W and W_0 are the total volume after and before the change, respectively (Supporting Information). As shown in Figure 2f and 2g, a simulation plot *via* COMSOL presents an electric potential difference between two electrodes in open-circuit condition (a constant value of triboelectric charge density of 2.0×10^{-6} C/m² on the FEP surface). Figure 2f illustrates the simulated maximum value of the electric potential difference (V_{oc}) versus ΔP, indicating a linear relationship in the range from 3.1 KPa to 12.2 KPa. Then, the V_{oc} reaches saturation when the pressure exceeds the linear range.

To quantify the performance of an M-TES, a motor (LinMot, Inc.) that can provide linear reciprocating motion was used to drive a syringe in connection to the air-conducting channel of the device. As revealed in **Figure 3**a, a periodic change of air pressure ($\Delta P = 7.1$ KPa) at a frequency of 0.3 Hz generates an oscillating voltage signal around 14.5 V at the same frequency. Different ranges of ΔP result in diverse voltage signals. As illustrated in Figure 3b, a minor V_{oc} of 0.2 V is obtained when ΔP is 3.1 KPa. If the air pressure changes in a wider range ($\Delta P = 9.4$ KPa), the V_{oc} shoots to 20.4 V, which is because larger ΔP expands the deformation of the membrane, thus an enhanced output voltage signal can be expected. Consistent with the simulated results, saturation occurs when ΔP is beyond 9.9 KPa, which indicates that the device reaches its detection limit. Such a saturation is caused by the reason that the deformation of the membrane has reached its elastic limit, which makes triboelectric charges on the membrane have little influence on the electric field distribution around electrodes.[26] An approximately linear relationship ($R^2 = 0.98$) between V_{oc} and ΔP can be realized by the M-TES when ΔP ranges from 3.1 KPa to 9.4 KPa, corresponding to an average sensitivity of 3.2 V/KPa. Since the Root Mean Square (RMS) of the noise (V_{noise}) at 1 Hz is 1.1 mV (Figure S3), the air pressure resolution at bandwidth of 1 Hz (ΔS) can be calculated to be 0.34 Pa by the following equation:

www.MaterialsViews.com

ADVANCED
FUNCTIONAL
MATERIALS
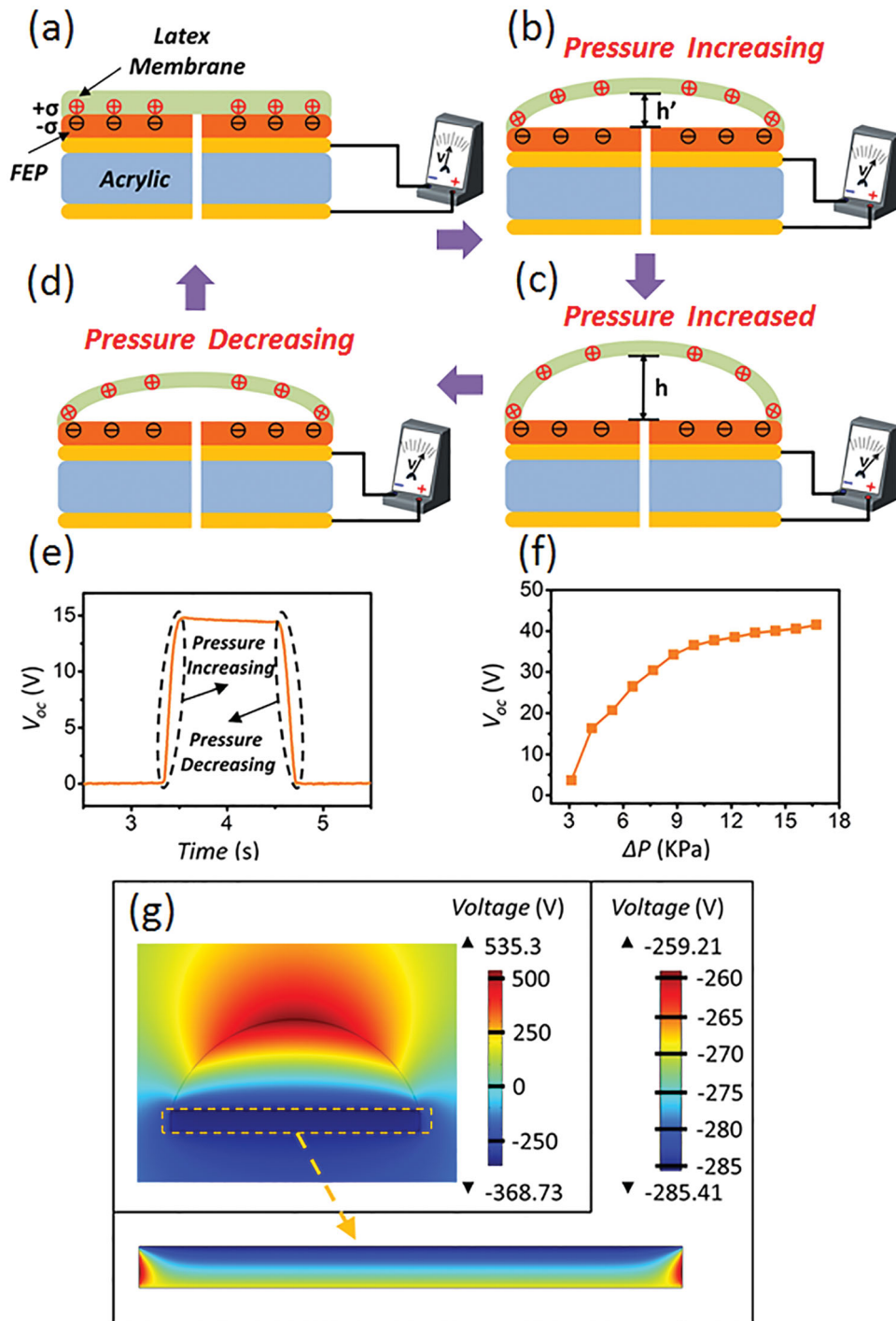www.afm-journal.de

FULL PAPER

Figure 2. Working principle of the M-TES in open-circuit condition. (a) The initial state, (b) separation of the charged surfaces, (c) fully separated position and (d) the two surfaces are approaching to each other. (e) Enlarged view of the output voltage signal. (f) Simulated results of V_{oc} versus the air pressure (g) COMSOL simulation results of the electric potential distribution when the two surfaces are separating from each other, enlarged view is the potential distribution on the electrodes (a constant value of triboelectric charge density of 2.0×10^{-6} C/m^2 on the contact surfaces).

$$\Delta S = \Delta p V_{noise} / \Delta V \qquad (2)$$

where ΔV is the output voltage signal in response to the air pressure change Δp. Such a resolution is almost 10 times higher than average commercialized products,[28] and even the contact pressure caused by a falling feather (~0.4 Pa)[13] is larger than it.

Integrated with a cavity (Figure S4), the M-TES is also applicable when the air pressure decreases. As displayed in Figure 3c, relative separation between latex and FEP lead to an output voltage signal of 12.0 V when ΔP is −2.3 KPa. Larger decrease of air pressure creates larger separation between the two contact materials and thus generates a higher output voltage. A similarly
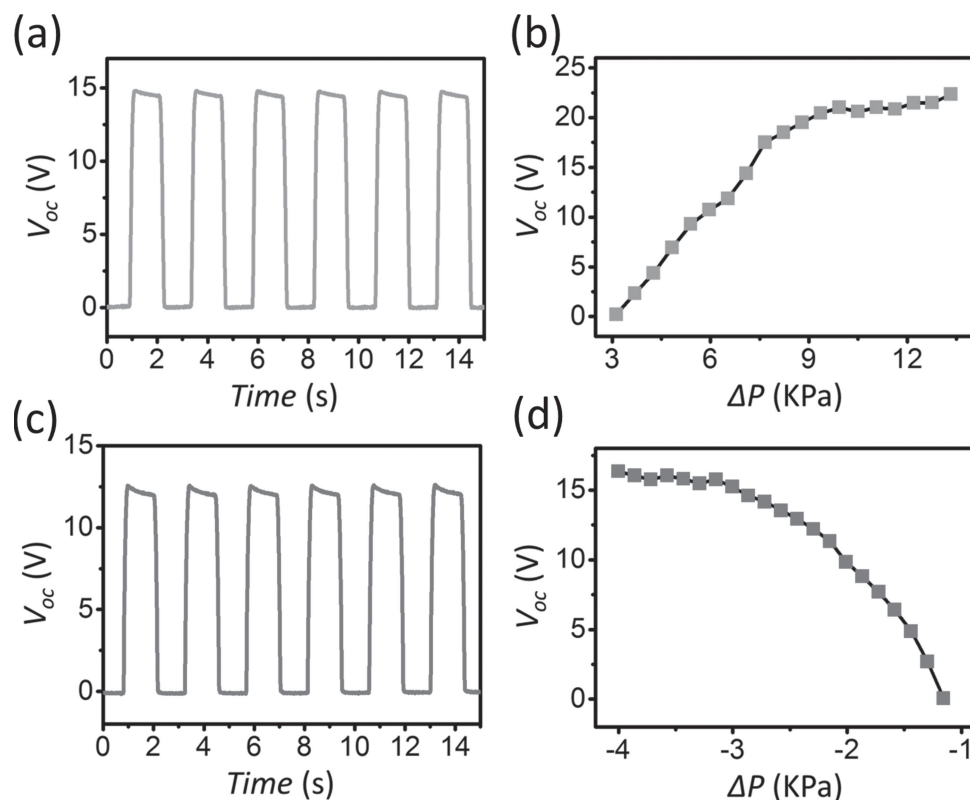
Figure 3. (a) V_{oc} of the M-TES when air pressure increases. (b) Dependence of V_{oc} on the increased air pressure. (c) V_{oc} of the M-TES when air pressure decreases. (b) Dependence of V_{oc} on the decreased air pressure.

linear relationship between the V_{oc} and ΔP can be achieved in Figure 3d in which the V_{oc} increases from 0.06 V to 15.8 V when ΔP decreases from -1.2 KPa to -3.5 KPa. Moreover, the output signal also reaches saturation around 16 V once ΔP is below -3.2 KPa. Therefore, the M-TES can be generally utilized when the pressure changes in other way with a sensitivity of 6.9 V/KPa, corresponding to a higher resolution of 0.16 Pa.

For structural optimization, the relationship between the sensitivity and the dimension of the M-TES is investigated. Output voltage signals from M-TESs with different circular apparent areas of 7.3 cm², 3.2 cm², and 0.8 cm² are measured when the air pressure changes in a small range (2.3 KPa < ΔP < 6 .2 KPa). As shown in **Figure 4**a, the M-TES with an apparent areas of 7.3 cm² exhibits an excellent linear relationship
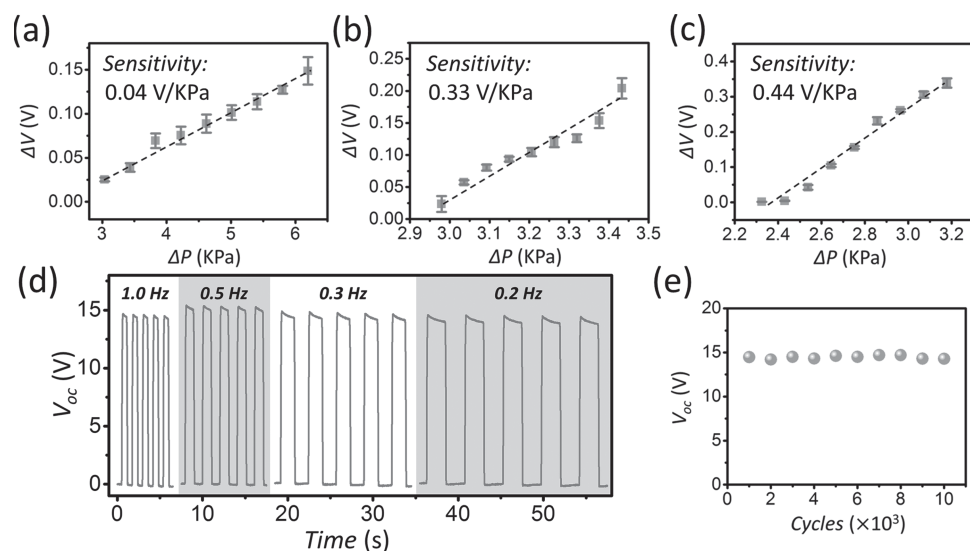

Figure 4. (a) Sensitivity of an M-TES with an effective contact area of 7.3 cm². (b) Sensitivity of an M-TES with an effective contact area of 3.2 cm². (c) Sensitivity of an M-TES with an effective contact area of 0.8 cm². (d) V_{oc} of M-TES when air pressure periodically changed from 101.3 KPa to 108.4 KPa at different frequencies. (e) Stability of the M-TES after longtime operation.
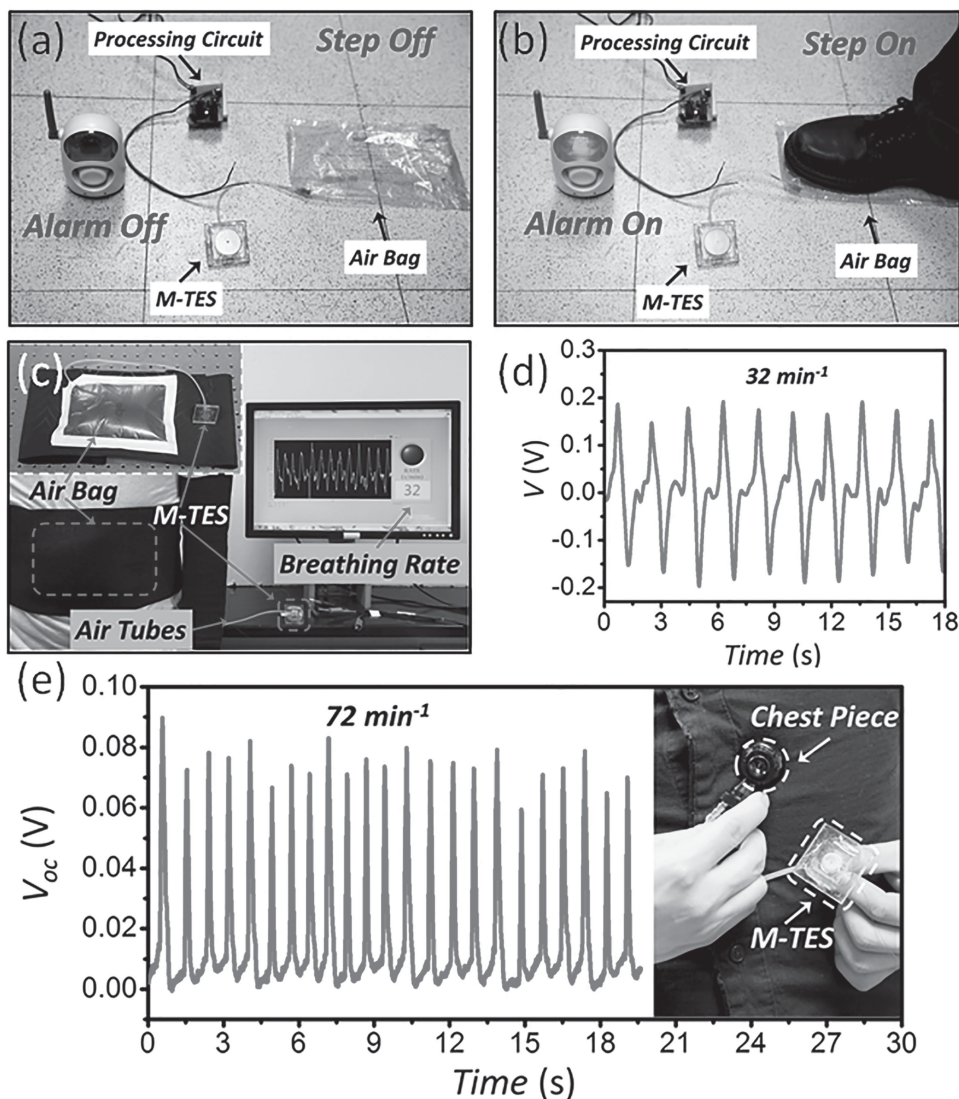
www.MaterialsViews.com

ADVANCED
FUNCTIONAL
MATERIALS
www.afm-journal.de

FULL PAPER

Figure 5. (a) Setup of a wireless security system, and the alarm has been triggered when (b) step on the air bag. (c) Demonstration of respiration detection by utilizing the M-TES. (b) Output voltage signals of the M-TES at a breathing rate of 32 times per minute. (e) Output voltage signals of the M-TES as a heartbeat monitor, insert: setup of the M-TES as a heartbeat monitor.

($R^2 = 0.98$) between its output voltage (ΔV) and ΔP. The ΔV goes ups from 0.02 V to 0.15 V when ΔP increases from 3.0 KPa to 6.2 KPa, corresponding to a linear fitting curve that can be expressed as

$$\Delta V = 0.04\Delta P - 0.08 \tag{3}$$

Thus, the average sensitivity of the M-TES is 0.04 V/KPa. Likewise, good linear relationships between ΔV and ΔP can also be obtained in M-TESs with smaller apparent areas of 3.2 cm^2 ($R^2 = 0.95$) and 0.8 cm^2 ($R^2 = 0.98$). However, sensitivities of M-TESs vary with apparent areas. According to Figure 4b and 4c, a sensitivity of 0.33 V/KPa when ΔP changes from 2.9 KPa to 3.4 KPa can be achieved by an M-TES with an apparent area of 3.2 cm^2, while a higher sensitivity of 0.44 V/KPa in the range from 2.3 KPa to 3.2 KPa can be achieved by an M-TES with a smaller apparent area of 0.8 cm^2. Such an effect of the apparent area on

the sensitivity of an M-TES can be explained by the reason that larger deformation of the membrane occurs for the device with smaller circular apparent area within the same range of pressure change. As a result, a higher sensitivity can be expected if a smaller device is used. It is to be noted that the sensitivity of the M-TES for a small range of ΔP differs from that for a large range since the separation between the membrane and the FEP is not linearly dependent on the pressure change. In addition, smaller apparent area reduces the elastic limit of the membrane, resulting in a decreased detection limit of an M-TES. Furthermore, to investigate possible impacts on the electric output signal of an M-TES from the frequency of the air pressure change, the V_{oc} of an M-TES with an apparent area of 3.2 cm^2 is measured when air pressure periodically changes (ΔP = 7.1 KPa) at different frequencies. It can be concluded from Figure 4d that the frequency has little impact on output signals of M-TES when the frequency reduces from 1.0 Hz to 0.2 Hz.

This is due to the fact that the V_{oc} depends on the static position of the membrane, which is independent of the dynamic frequency. Moreover, the stability of the M-TES was investigated by long-time operation under the circumstance where air pressure periodically changed (ΔP = 7.1 KPa) at a frequency of 0.3 Hz. After 10,000 cycles (Figure S5), the output voltage signal still keeps constant around 14.5 V (Figure 4e), which indicates a strong stability of the M-TES.

To demonstrate the ability of M-TESs as active air pressure sensors, three sets of practical applications were demonstrated. As demonstrated in **Figure 5**a, a wireless security system is built by integrating an M-TES, an air bag (12 × 18 × 1 cm), a processing circuit (Figure S6), and a safety alarm (Home Safe, Inc.). The M-TES was able to generator a voltage signal due to a pressure change when the air bag is pressed; and such a voltage signal could trigger the security alarm though the processing circuit (Figure 5b, Video S1 in Supporting Information). Compared to traditional technologies, the M-TES can provide a simple and reliable way to achieve a security monitoring system or a motion detection technology. Air pressure sensors can be utilized for respiration detection in various fields such as medicine and nursing.[28] Here in this work, we demonstrate a simple and low-cost system for respiration detection by using M-TESs. As sketched inserted in Figure 5c, an air bag (18 × 22 × 1 cm) with air tubes was connected with an M-TES. An adjustable back brace is used to attach the air bag to the abdomen of a subject. The abdominal expansion and contraction of respiratory activity will result in a periodical air pressure change in the air bag which can be detected by the M-TES. Once the respiratory movement occurs, output voltage signals generated by the M-TES will be collected by a program developed by LabView; and the average breathing rate in real time displays on the monitor (Figure 5c). Electric signals indicate a breathing rate of 32 times per minute when the subject carries on a normal breathing rate (Figure 5d). Inspirations caused by pulmonary expansion are shown as maxima peaks, while expirations caused by pulmonary contraction are shown as minima ones (see Video S2 in Supporting Information). Heartbeat monitors has been largely used by performers of various types of physical exercise and medical purposes. Due to the high resolution, we successfully demonstrate a heartbeat monitor based on the M-TES. Air pressure change in a chest piece is caused by the heartbeat transmit *via* air-filled hollow tubes to the M-TES (inserted in Figure 5e). Such a periodical air pressure change will result in output voltage signals for the M-TES. In such a case, each heartbeat can be recorded by a pulse signal. The output voltage signals around 0.06 V in Figure 5e shows that the test subject has a stable heartbeat rate of 72 times per minute which is consistent with the counting result. Therefore, in our proposed method, the obtained breathing and heartbeat rate can be successfully obtained by output voltage signals, which can be applied for easy handling detection systems required for daily home use.

3. Conclusion

In summary, we demonstrate membrane-based triboelectric sensors as self-powered air pressure sensors with extremely high resolutions for surveillance and health Monitoring. The small-sized and light-weighted M-TES provides an effective way to detect the air pressure change for circumstances when air pressure increases or decreases. The device shows strong stability after longtime operation, and higher sensitivity can be expected when the device is further miniaturized. Furthermore, output voltage signals can be directly utilized for air pressure sensing, frequency monitoring, and other practical applications. Given its good linearity, easy fabrication process and low cost, the M-TES presented in this work can be further applied for water depth sensing, health monitoring as well as for other self-powered monitoring systems.

Supporting Information

Supporting Information is available from the Wiley Online Library or from the author.

Acknowledgements

[1] S. J. Pearton, B. S. Kang, S. Kim, F. Ren, B. P. Gila, C. R. Abernathy, J. Lin, S. N. G. Chu, *J. Phy.: Condens. Matter.* **2004**, *16*, R961.

[2] A. Lloyd Spetz, A. Baranzahi, P. Tobias, I. Lundström, *Phys. Status Solidi A* **1997**, *162*, 493.

[3] J. Kim, F. Ren, B. P. Gila, C. R. Abernathy, S. J. Pearton, *Appl. Phys. Lett.* **2003**, *82*, 739.

[4] S. Roy, S. Basu, *B. Mater. Sci.* **2002**, *25*, 513.

[5] A. Kooser, R. L. Gunter, W. D. Delinger, T. L. Porter, M. P. Eastman, *Sensor. Actuat. B-Chem.* **2004**, *99*, 474.

[6] C. S. Sander, J. W. Knutti, J. D. Meindl, *IEEE T. Electron. Dev.* **1980**, *27*, 927.

[7] P. A. Snow, E. K. Squire, P. S. J. Russell, L. T. Canham, *J. Appl. Phys.* **1999**, *86*, 1781.

[8] Z. L. Wang, W. Wu, *Angew. Chem., Int. Ed.* **2012**, *51*, 11700.

[9] Z. L. Wang, J. Song, *Science* **2006**, *312*, 242.

[10] Z. L. Wang, *Sci. Am.* **2008**, *298*, 82.

[11] I. F. Akyildiz, J. M. Jornet, *Nano Commun. Networks* **2010**, *1*, 3.

[12] F.-R. Fan, L. Lin, G. Zhu, W. Wu, R. Zhang, Z. L. Wang, *Nano Lett.* **2012**, *12*, 3109.

[13] J. Chen, G. Zhu, W. Yang, Q. Jing, P. Bai, Y. Yang, T. C. Hou, Z. L. Wang, *Adv. Mater.* **2013**, *25*, 6094.

[14] Z.-H. Lin, G. Zhu, Y. Zhou, Y. Yang, P. Bai, J. Chen, Z. L. Wang, *Angew. Chem.* **2013**, *19*, 5065.

[15] F.-R. Fan, Z.-Q. Tian, Z. L. Wang, *Nano Energy* **2012**, *1*, 328.

[16] B. Meng, W. Tang, X. S. Zhang, M. D. Han, W. Liu, H. X. Zhang, *Nano Energy* **2013**, *6*, 1101.

[17] S. Wang, L. Lin, Z. L. Wang, *Nano Lett.* **2012**, *12*, 6339.

[18] P. Bai, G. Zhu, Y. Liu, J. Chen, Q. Jing, W. Yang, J. Ma, G. Zhang, Z. L. Wang, *ACS Nano* **2013**, *7*, 6361.

FULL PAPER

[19] G. Zhu, J. Chen, T. Zhang, Q. Jing, Z. L. Wang, *Nat. Commun.* **2014**, *5*, 3426.

[20] G. Zhu, Z.-H. Lin, Q. Jing, P. Bai, C. Pan, Y. Yang, Y. Zhou, Z. L. Wang, *Nano Lett.* **2013**, *13*, 847.

[21] P. Bai, G. Zhu, Z.-H. Lin, Q. Jing, J. Chen, G. Zhang, J. Ma, Z. L. Wang, *ACS Nano* **2013**, *7*, 3713.

[22] H. Fang, W. Wu, J. Song, Z. L. Wang, *J. Phys. Chem. C* **2009**, *113*, 16571.

[23] A. F. Diaz, R. M. Felix-Navarro, *J. Electrostat.* **2004**, *62*, 277.

[24] F. Saurenbach, D. Wollmann, B. D. Terris, A. F. Diaz, *Langmuir* **1992**, *8*, 1199.

[25] L. H. Lee, *J. Electrostat.* **1994**, *32*, 1.

[26] S. Niu, Y. Liu, S. Wang, L , Lin, Y. Zhou, Y. Hu, Z. L. Wang, *Adv. Funct. Mater.* **2014**, *24*, 3332.

[27] Y. Yang, Y. S. Zhou, H. Zhang, Y. Liu, S. Lee, Z. L. Wang, *Adv. Mater.* **2013**, *25*, 6594.

[28] K. Ho, N. Tsuchiya, H. Nakajima, K. Kuramoto, S. Kobashi, Y. Hata, *Proc. 2009 IEEE Int. Conf. Fuzzy Systems* **2009**, 911.